

# Embodied Image Quality Assessment for Robotic Intelligence

Jianbo Zhang<sup>1</sup>, Chunyi Li<sup>1</sup>, Liang Yuan<sup>2</sup>, Guoquan Zheng<sup>3</sup>, Jie Hao<sup>3</sup>, Guangtao Zhai<sup>1</sup>, *Fellow, IEEE*

<sup>1</sup>Institute of Image Communication and Network Engineering, Shanghai Jiao Tong University

<sup>2</sup>USC-SJTU Institute of Cultural and Creative Industry, Shanghai Jiao Tong University

<sup>3</sup>College of Information Science and Technology, Beijing University of Chemical Technology

**Abstract**—Image quality assessment (IQA) of user-generated content (UGC) is a critical technique for human quality of experience (QoE). However, for robot-generated content (RGC), will its image quality be consistent with the Moravec paradox and counter to human common sense? Human subjective scoring is more based on the attractiveness of the image. Embodied agent are required to interact and perceive in the environment, and finally perform specific tasks. Visual images as inputs directly influence downstream tasks. In this paper, we first propose an embodied image quality assessment (EIQA) frameworks. We establish assessment metrics for input images based on the downstream tasks of robot. In addition, we construct an Embodied Preference Database (EPD) containing 5,000 reference and distorted image annotations. The performance of mainstream IQA algorithms on EPD dataset is finally verified. The experiments demonstrate that quality assessment of embodied images is different from that of humans. We sincerely hope that the EPD can contribute to the development of embodied AI by focusing on image quality assessment. The benchmark is available at [https://github.com/Jianbo-maker/EPD\\_benchmark](https://github.com/Jianbo-maker/EPD_benchmark).

**Index Terms**—Image quality assessment, embodied AI, EPD

## I. INTRODUCTION

Over the past two decades, Image Quality Assessment (IQA) has undergone significant evolution, with traditional methods aiming to mimic the Human Visual System (HVS) in image observation. However, Embodied Artificial Intelligence (EAI) faces an open challenge: understanding how image quality impacts the performance of embodied tasks. Unlike traditional assessment methods, which are limited to evaluating single, static images, EAI underscores the importance of interaction and perception within an environment. Robots perform specific tasks through interaction with their surroundings, where the image quality is crucial in determining the success of these tasks. Most approaches are offline and modular. They concentrate solely on assessing individual image quality, without considering the context of the robotic specific tasks. The robotics community has increasingly focused on the development of denoising algorithms for different types of image noise, including rain and fog removal, customized for specific environmental conditions. The development of a robot-centric evaluation methodology for embodied agents is of paramount importance for the integrated advancement of the Deep Learning (DL) technology and the robotic technology.

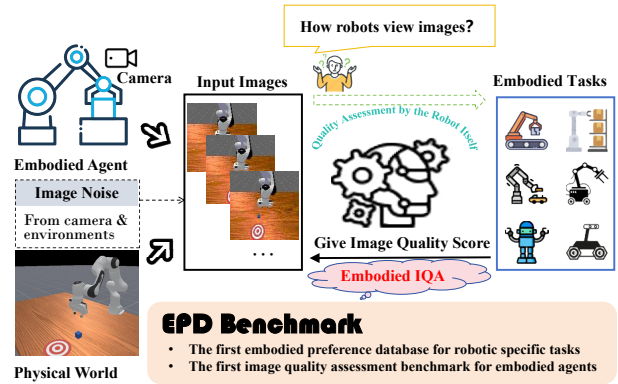


Fig. 1: Input image quality is assessed based on the performance of the robot for embodied tasks. The EPD benchmark benefit image quality assessment for EAI.

There are inherent disparities between the human visual system and the Robot Visual System (RVS). Generally, humans prioritize the high-level semantic content of an image, whereas machines tend to analyze the low-level geometric structure. For example, in the context of a robotic task, the distortion of image luminance variation has a lesser impact on its ability to perform tasks, in contrast to the significant detriment caused by spatial distortion. Consequently, robots prioritize the consistency of image texture and structure and are less sensitive to changes in semantic information, which contrasts with human perceptions of image quality.

Vision-based embodied artificial intelligence has a wide range of research prospects. However, a comprehensive framework for assessing the image quality of robotic vision systems remains undeveloped. The application of vision technology to robotics itself has inherent limitations. Vision cameras are passive sensors that passively receive information from the environment. The camera itself and its surroundings are subject to a large number of interfering factors, especially in the image collection and transmission where additional noise is introduced. Embodied intelligence designed only through ideal images is difficult to interact with the real world. The primary bottleneck hindering this research is the absence

of image quality assessment for embodied AI. Considering this, this paper proposes a benchmark for quality assessment of embodied images, Fig. 1 illustrates the paradigm of the proposed benchmark. Our main contributions are as follows:

- We introduce a standardized procedure for collecting subjective labels from embodied robots. We innovatively define the subjective preferences of Embodied AI. The impact of varying image quality inputs on the robotic downstream tasks is assessed.
- We construct the embodied preference database EPD, which is the first IQA database for embodied AI. This database comprises 2,500 reference/distorted image pairs. The images are annotated via a robotic arm completing some embodied tasks. The EPD explore the internal mechanism of IQA in embodied AI.
- We benchmarked existing IQA methods in the EPD database. The experimental results validated the existence of inconsistency between HVS and RVS.

## II. RELATED WORK

### A. Image Quality Assessment

Human-oriented image quality assessment methods can be divided into three categories, the Full-Reference (FR) IQA, the Reduced-Reference (RR) IQA, and the No-Reference (NR) IQA. The FR IQA method assumes that a distortion-free reference image exists and that the reference image information is fully available [1]–[3]. The RR IQA method usually assesses the quality of an image using partial information from a reference image or extracting a small number of features [4]. The NR IQA approach usually refers to the assessment of distorted image quality in the absence of the original distortion-free image [5], [6].

In addition, the benchmark for image quality assessment is a crucial issue [7], [8]. Previous work has modelled the human visual system for image quality assessment. However, there are differences in humans and embodied robots view images. To the best of our knowledge we present the first image quality assessment for Embodied Artificial Intelligence.

### B. Embodied Artificial Intelligence

In contrast to traditional deep learning methods, embodied artificial intelligence emphasises the exploration of the surrounding environment by an intelligent agent, which is subject to active perception, interaction and reasoning. Existing work studies embodied intelligence from a number of different perspectives, such as embodied agent, embodied simulators, embodied perception, embodied interaction [?], [9]–[13].

As with the development of traditional AI, embodied AI also requires a large amount of experimental data and scenarios for testing. A simulator can simulate the real physical world, subject to the limitations of experimental conditions and considerations of experimental safety. The Issac Sim [14], Gazebo [15], and PyBullet [16] provide a general-purpose simulator to support algorithm development and model training. Simulators such as AI2-THOR [17], Habitat [18], SAPIEN [19]. These platform provide a large number of scenarios that simulate

real-world, task-specific scenarios, including virtual scenes and virtual objects. In this paper, the SAPIEN is used as a simulation environment to evaluate the image quality by using a robotic arm to perform specific tasks.

## III. DATABASE CONSTRUCTION

### A. Image Collection

In contrast to traditional IQA image collection methods, embodied AI requires interaction with the surrounding environment. The ultimate goal is robot-oriented image quality assessment, and thus, image collection is also done by the robot itself. Two classical reinforcement learning algorithms, the Proximal Policy Optimization (PPO) [20] and the Soft Actor-Critic (SAC) [21], and a state-of-the-art method, TDMPC2 [22], are used to perform the 2 tasks in the SAPIEN simulator [19], respectively. A monocular camera is used to capture RGB images as sensor data input to the model.

For distorted images, 25 common types of image distortions are set by modelling the image inputs by simulating camera noise and environmental noise. Specifically, these image distortion types are classified into 7 categories are Blus distortions, Colour distortions, Compression, Noise, Brightness change, Spatial distortions, Sharpness and contrast. A embodied task requires multiple images to work together, but the image distortion type is set to be consistent. Therefore, only the image of the initial frame is selected as the image to be evaluated. For a more extensive evaluation, 100 different initial scenes are set for each task separately. In summary, a total of 5,000 reference and distorted images are collected for the database. The construction overview of the proposed EPD benchmark is shown in Fig. 2.

### B. Preference Score Collection

Based on a simulated environment, a robotic arm acts as an embodied intelligence to perform simple push and pick tasks. For the robot, different quality of image inputs have different impacts on the robot to complete the task, which is also directly related to the performance of the robot. Based on the ManiSkill platform [23], three reinforcement learning algorithms are used to complete two different tasks of push and pick boxes in the same scene. The reward value of each episodes is adopted as the performance score for evaluating the robot performance in the process of perceiving the environment and completing the embodied intelligence task. The robotic arm perceives the surrounding environment, then makes decisions based on the perception results, and finally executes the corresponding actions.

For the PPO algorithm [20], the goal of the robot is to find a policy parameter  $\theta$  that maximises the expected cumulative reward. The reward function  $r(\mathbf{s}_t, \mathbf{a}_t)$  represents the immediate reward obtained by the agent performing action  $\mathbf{a}_t$  in state  $\mathbf{s}_t$  at time step  $t$ . PPO maximises the cumulative reward in the environment by optimising the policy  $\pi_\theta$ . The expectation of the cumulative reward  $J(\theta)$  is denoted as:

$$J(\theta) = E_{\tau \sim \pi_\theta(\tau)} \left[ \sum_{t=1}^T r(\mathbf{s}_t, \mathbf{a}_t) \right], \quad (1)$$

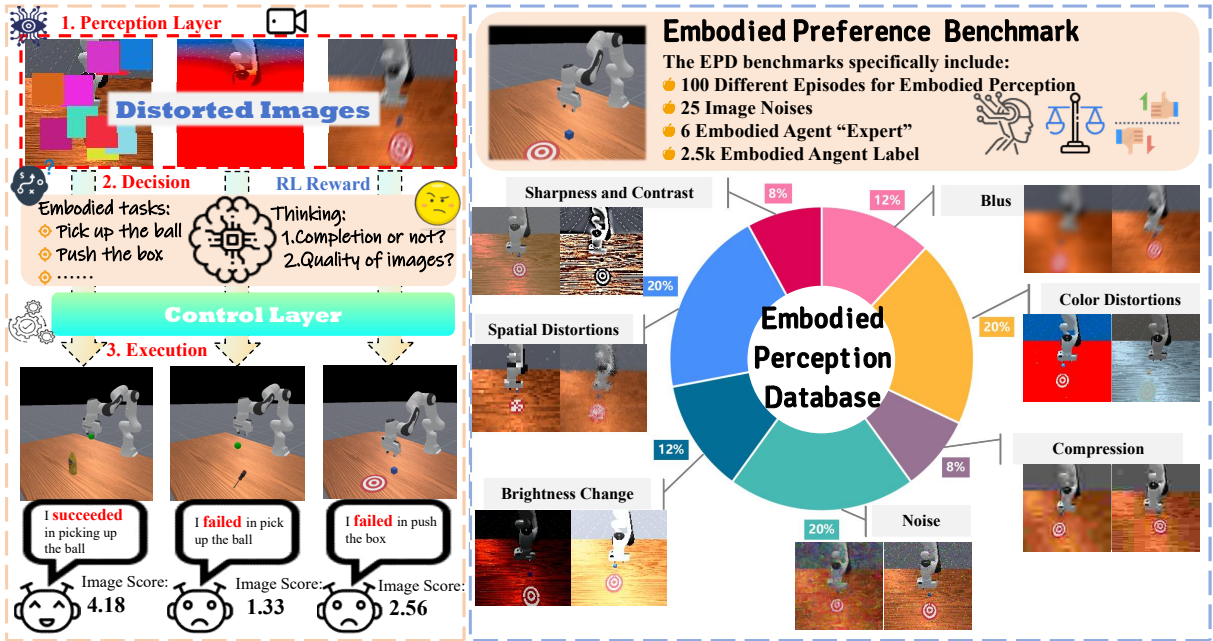


Fig. 2: The construction overview of the proposed EPD Benchmark. The EPD benchmark is oriented towards embodied AI and includes 25 common image distortions. There are 100 pairs of reference/distortion images for each distortion type.

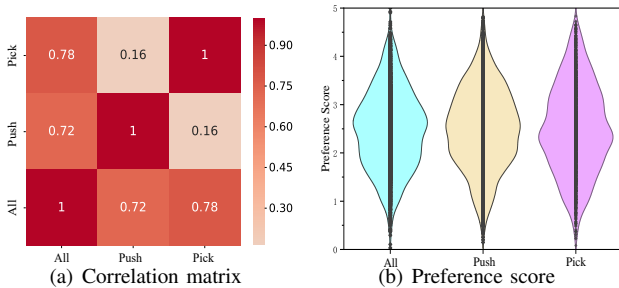


Fig. 3: The dataset analyses of EPD. (a) The correlation matrix for MOS. It is the correlation analyses for the subsets of the all task, the push task and the pick task respectively. (b) The distribution of normalized data. It can be seen that the data distribution is similar among different tasks.

where the  $E_{\tau \sim \pi_{\theta}(\tau)}[\cdot]$  denotes the expected value of the cumulative reward  $r(\tau)$  for all possible trajectories  $\tau$  (i.e., sequences of states and actions). In addition, the trajectory  $\tau$  is generated by the strategy  $\pi_{\theta}$ .

The SAC [21] method introduces an entropy regularisation term in reinforcement learning to encourage the agent to explore more actions. The reward function of SAC contains not only the immediate reward of the environmental feedback but also the entropy value of the current strategy in order to balance the exploration with the expected reward. Denote immediate reward from  $s_t$  to  $s_{t+1}$  as  $R(s_t, a_t, s_{t+1})$ . Given the  $H(\pi(\cdot | s_t))$  denotes the entropy of the strategy  $\pi$  in state  $s_t$ .

We denote the expectation reward function of SAC as  $\pi^*$ :

$$\pi^* = \arg \max_{\pi} E_{\tau \sim \pi} \left[ \sum_{t=0}^{\infty} \gamma^t (R(s_t, a_t, s_{t+1}) + \alpha H(\pi(\cdot | s_t))) \right], \quad (2)$$

where  $\gamma^t$  is scale factor, and  $\alpha$  is entropy regularisation factor.

TDMPC2 [22] derives its closed-loop control strategy by planning with the learnt world model. The agent utilises the model to predict future states and selects the optimal sequence of actions based on the predictions. We denote  $D(s_{t+1}, s_{\text{goal}})$  as the distance between  $s_{t+1}$  and  $s_{\text{goal}}$ . Therefore, the reward function of TDMPC2  $W(s_t, a_t, s_{t+1})$  is:

$$W(s_t, a_t, s_{t+1}) = r(s_t, a_t) + \lambda \cdot D(s_{t+1}, s_{\text{goal}})^{-1}, \quad (3)$$

where  $\lambda$  is the weight factor.

Each episodes receives a reward corresponding to the score of the image, and finally the embodied Mean Opinion Score (MOS) are normalised to the range (0, 5).

#### IV. DATABASE ANALYSIS

The MOS of the EPD and the subscores of the two tasks are shown in Fig. 3, and their correlation is quantified by the Spearman Rank Order Correlation Coefficient (SRCC). As can be seen from the figure, the correlation between tasks is low. Since the difficulty of both push and pick tasks is different, the reward values for the tasks are also different. The data distributions for the two tasks and the total MOS are similar, both showing an approximate normal distribution. In addition, there is a strong correlation between the overall scores and the individual tasks, with all SRCC exceeding 0.5. The EPD dataset is reliable in this category of tasks.

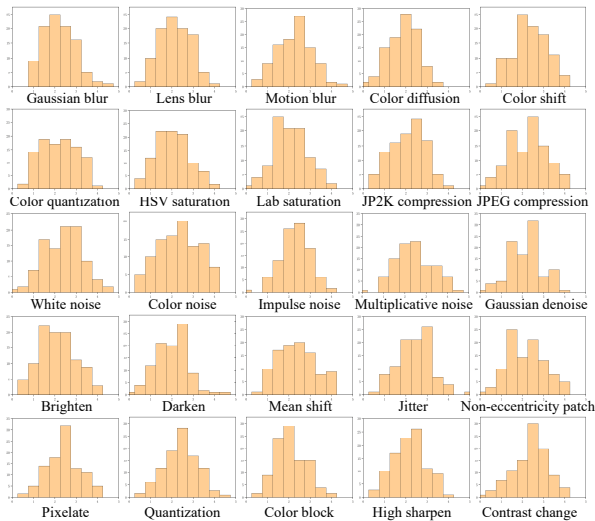


Fig. 4: MOS score of the EPD, visualized in 25 distortion subsets. The results show the reflection of different image distortion in the perspective of the robot.

Fig. 4 illustrates the MOS distribution of the 25 distortions. From the results, it can be seen that the assessment of an image by a robot is not the same as the assessment of an image by a human. Robots are not as sensitive as humans to changes in brightness when performing tasks. The distortions in sharpness and contrast have a greater impact on robots. Essentially, embodied robots focus on the low-level pixel-level features of an image, while humans focus on the high-level semantic features of an image. Therefore, the type of distortion that affects the pixel features can seriously affect the embodied task, whereas the type of distortion that destroys the semantic integrity, which is more of a concern to the human visual system, only affects the image assessment of humans. Hence the method of image quality assessment that based on human visual system is not work well.

## V. EXPERIMENT

This section describes the setup of the experiment, then analyses the environment of the experiment, and finally evaluates the results of the experiment.

### A. Experiment Setups

Oriented to the 100 episodes of the embodied task, 25 common image distortions are set up, and a total of 2,500 distorted images as well as the corresponding reference images are acquired. The train/val dataset is divided according to an 8:2 ratio. For each pair of images the overall scoring and the score of the two subtasks is annotated. Three metrics, SRCC, Kendall Rank Order Correlation Coefficient (KRCC) and Pearson Linear Correlation Coefficient (PLCC), are used to evaluate the consistency between objective and subjective quality scores. Where SRCC and KRCC represent predictive monotonicity and PLCC represents predictive accuracy.

| Reference | Distortion  | Reference | Distortion  |
|-----------|-------------|-----------|-------------|
|           |             |           |             |
| RF-1-83   | Score: 2.97 | RF-8-209  | Score: 4.07 |
|           |             |           |             |
| RF-9-89   | Score: 3.41 | RF-13-2   | Score: 1.62 |
|           |             |           |             |
| RF-17-95  | Score: 3.20 | RF-24-299 | Score: 4.01 |

Fig. 5: The first and third columns are the reference images, and the second and fourth columns correspond to the distorted images and scores. RF-X-X denotes the file name of the example image in the EPD benchmark.

For algorithm evaluation, we utilize 14 mainstream IQA methods for the comparison. These methods have achieved commendable results in terms of IQA methods based on the human visual system. In addition to comparing traditional PSNR and SSIM [1], the full reference IQA methods include AHQ [24], PieAPP [25], CKDN [26], DISTS [27], TOPIQFR [28], IQT [29]. The no reference methods include CLIPIQA [30], DBCNN [31], TOPIQNR [28], MANIQA [32], TempQT [33], HyperIQA [34]. We trained 12 algorithms on the EPD dataset based on the PyIQA [35] platform, following the data division described above. Instead of fixing the epoch during training, the models are trained until the loss converged relatively. We evaluated each algorithm on three evaluation metrics on three subdatasets. The hardware platform on which the experiments is 8×NVIDIA RTX3090 24G GPUs.

### B. Environment Setups

It is important to note that the EPD benchmark is different from the traditional paradigm. Instead of offline collection of various types of images, the EPD are oriented towards a real scenario with embodied AI. A robot needs to constantly perceive its surroundings as it completes its task. We capture images from a monocular camera mounted on the robot as it performs its task. Thus, the collected images are primarily for the robot and not for humans.

For the experiments, the ManiSkill benchmark [23] was chosen to set up the experimental environment, which is a development platform for reinforcement learning tasks and imitation learning with embodied intelligence based on the SAPIEN simulator [19]. The experiment is set up with two subtasks of pushing and picking a box, and the goal is to complete the specified tasks through reinforcement learning,

Table I. Comparison of 14 IQA methods for BL (Baseline), FR (Full Reference), NR (No reference) respectively on EPD benchmarks. **Bold** represent the best results in BL. In FR and NR, the Best results are marked in **Orange** while the second best results are in **Blue**.

| Type | Metric                   | All Tasks       |                 |                 | Push Task       |                 |                 | Pick Task       |                 |                 |
|------|--------------------------|-----------------|-----------------|-----------------|-----------------|-----------------|-----------------|-----------------|-----------------|-----------------|
|      |                          | SRCC $\uparrow$ | PLCC $\uparrow$ | KRCC $\uparrow$ | SRCC $\uparrow$ | PLCC $\uparrow$ | KRCC $\uparrow$ | SRCC $\uparrow$ | PLCC $\uparrow$ | KRCC $\uparrow$ |
| BL   | PSNR                     | <b>0.1233</b>   | <b>0.1356</b>   | <b>0.0819</b>   | <b>0.0811</b>   | <b>0.0927</b>   | <b>0.0539</b>   | <b>0.0972</b>   | <b>0.1138</b>   | <b>0.0645</b>   |
|      | SSIM (TIP2004) [1]       | 0.0597          | 0.0635          | 0.0396          | 0.0633          | 0.0716          | 0.0417          | 0.0228          | 0.0275          | 0.0152          |
| FR   | PieAPP (CVPR2018) [25]   | 0.3616          | 0.3853          | 0.2466          | 0.1727          | 0.2023          | 0.1165          | 0.1604          | 0.1802          | 0.1061          |
|      | CKDN (ICCV2021) [26]     | <b>0.6971</b>   | <b>0.6654</b>   | <b>0.5062</b>   | 0.2100          | 0.2186          | 0.1404          | <b>0.3372</b>   | 0.3040          | <b>0.2266</b>   |
|      | IQT (CVPR2021) [29]      | <b>0.5435</b>   | <b>0.5416</b>   | <b>0.3814</b>   | <b>0.3918</b>   | <b>0.3706</b>   | <b>0.2650</b>   | <b>0.5613</b>   | <b>0.5664</b>   | <b>0.3920</b>   |
|      | AHIQ (CVPR2022) [24]     | 0.4199          | 0.4382          | 0.2888          | <b>0.2425</b>   | <b>0.2707</b>   | <b>0.1674</b>   | 0.3061          | <b>0.3157</b>   | 0.2074          |
|      | DISTS (TPAMI2022) [27]   | 0.2113          | 0.2107          | 0.1428          | 0.1335          | 0.1608          | 0.0906          | 0.1135          | 0.1036          | 0.0985          |
|      | TOPIQ-FR (TIP2024) [28]  | 0.1265          | 0.1232          | 0.0845          | 0.1615          | 0.1684          | 0.1113          | 0.1207          | 0.1185          | 0.0794          |
| NR   | HyperIQA (CVPR2020) [34] | <b>0.3212</b>   | <b>0.3289</b>   | <b>0.2212</b>   | <b>0.3099</b>   | <b>0.2981</b>   | <b>0.2098</b>   | <b>0.4055</b>   | <b>0.3927</b>   | <b>0.2733</b>   |
|      | DBCNN (TCSVT2021) [31]   | 0.1921          | 0.2133          | 0.1307          | 0.0962          | 0.1039          | 0.0643          | 0.1882          | 0.1855          | 0.1251          |
|      | MANIQA (CVPR2022) [32]   | <b>0.5267</b>   | <b>0.5603</b>   | <b>0.3675</b>   | <b>0.2475</b>   | <b>0.2574</b>   | <b>0.1661</b>   | <b>0.5847</b>   | <b>0.5859</b>   | <b>0.4116</b>   |
|      | CLPIQA (AAAI2023) [30]   | 0.1821          | 0.2160          | 0.1218          | 0.0750          | 0.0893          | 0.0503          | 0.1464          | 0.1497          | 0.0978          |
|      | TempQT (TMM2024) [33]    | 0.2340          | 0.1730          | 0.1450          | 0.1040          | 0.0980          | 0.0560          | 0.2210          | 0.1400          | 0.1500          |
|      | TOPIQ-NR (TIP2024) [28]  | 0.1253          | 0.1193          | 0.0828          | 0.0995          | 0.1043          | 0.0667          | 0.0846          | 0.0602          | 0.0568          |

i.e., pushing the box to the centre of the sign and picking the box. Each episodes represents one complete interaction of the robotic arm with the environment in different scenarios, and the experiment set 50 steps of actions for each episodes. Incidentally, reward values are given for each step.

To explore the capability of the robot to task completion under different distorted images, the type and intensity of noise set in an episodes is consistent. The final task completion performance is measured by the average reward value. Thus, it can score the images captured by the robot while completing the embodied task, and the scores of several distorted images are shown in Fig. 5. Limited by the size and computational resources of the available reinforcement learning models, the image inputs captured by the robot are all  $128 \times 128$  pixels.

### C. Experiment Results and Discussion

Table I demonstrates the performance of IQA methods on the EPD. As can be seen from the table, the traditional IQA methods based on the human visual system do not perform well in the IQA of the robot visual system. It also proves that the perspective of embodied robots is not consistent with the image assessment methods in human perspective. For image quality assessment from the robotic viewpoint the algorithms cannot be designed simply with the human visual system.

Current state-of-the-art methods can only achieve performance below 0.7. In the FR method, CKDN [26] and IQT [29] are able to achieve SRCC and PLCC above 0.5. In the NR method only MANIQA [32] is able to achieve SRCC and PLCC above 0.5. Overall, the full-reference FR methods perform slightly better than the NR methods. Existing methods are essentially modelling the human visual system, while less attention is paid to the robotic visual system. It is interesting to note that CKDN [26] obtains state-of-the-art results on the EPD benchmark. CKDN uses the results of Image Restoration (IR) as a reference image for model training. This also gives us some inspiration that in embodied AI it is *only the machine that understands the machine better*.

Table II. Comparison of MOS in different image distortion for 6 EAI participant. The D.1 to D.7 denote seven different types of image distortions, namely blus, colour distortions, compression, noise, brightness change, spatial distortions, sharpness and contrast. **Bold** data indicate the average best result.

| Dist | EAI_1         | EAI_2         | EAI_3         | EAI_4         | EAI_5         | EAI_6         | Mean          |
|------|---------------|---------------|---------------|---------------|---------------|---------------|---------------|
| D.1  | 3.5140        | 3.9556        | 2.7400        | 4.1523        | 2.6462        | 2.9477        | 3.3260        |
| D.2  | 3.4792        | 3.8651        | 2.9088        | 4.2066        | 2.7812        | 2.6387        | 3.3133        |
| D.3  | 3.4816        | <b>3.9790</b> | 3.0458        | 4.2192        | 2.8106        | 2.5506        | 3.3478        |
| D.4  | <b>3.5872</b> | 3.9600        | 2.8829        | 4.1867        | 2.7526        | <b>3.0249</b> | 3.3991        |
| D.5  | 3.5245        | 3.8871        | 2.9927        | 3.9267        | 2.7366        | 2.6478        | 3.2859        |
| D.6  | 3.4871        | 3.9393        | <b>3.0565</b> | <b>4.2275</b> | 2.7945        | 2.8989        | 3.4006        |
| D.7  | 3.4339        | 3.8575        | 3.0218        | 4.2242        | <b>2.9652</b> | 2.9357        | <b>3.4064</b> |

In addition, the performance of each method varies in different subtasks. The pick task has a higher performance than the push task, while the total task has the highest performance. EIQA still has significant optimisation space.

Table II shows the results of the average scores of distorted images from 6 different embodied AI participants. Each EAI assesses image quality differently in different image distortion environments. There are two participants each who scored high on noise and spatial distortion. One participant each scored the highest on compression, sharpness and contrast distortion. This also shows that there is variability in the image quality assessment by different EAI individuals.

## VI. CONCLUSION

This paper extends the IQA approach to embodied AI for the first time, and constructs the first robot-oriented image quality assessment database EPD. Experiments demonstrate that there is a gap between the robot vision system and the human vision system, and the current image quality assessment from the human perspective is limited. The application of embodied AI is strongly dependent on the input of visual images, and even far exceeds the human requirements for image quality. In future work, we intend to continue to expand the scope of

the embodied preference database to lay the foundation for the development of embodied AI.

## REFERENCES

- [1] Zhou Wang, A.C. Bovik, H.R. Sheikh, and E.P. Simoncelli, "Image quality assessment: from error visibility to structural similarity," *IEEE Transactions on Image Processing*, vol. 13, no. 4, pp. 600–612, 2004.
- [2] Wufeng Xue, Lei Zhang, Xuanqin Mou, and Alan C. Bovik, "Gradient magnitude similarity deviation: A highly efficient perceptual image quality index," *IEEE Transactions on Image Processing*, vol. 23, no. 2, pp. 684–695, 2014.
- [3] Jongyoo Kim and Sanghoon Lee, "Deep learning of human visual sensitivity in image quality assessment framework," in *2017 IEEE Conference on Computer Vision and Pattern Recognition (CVPR)*, 2017, pp. 1969–1977.
- [4] Guangtao Zhai, Xiaolin Wu, Xiaokang Yang, Weisi Lin, and Wenjun Zhang, "A psychovisual quality metric in free-energy principle," *IEEE Transactions on Image Processing*, vol. 21, no. 1, pp. 41–52, 2012.
- [5] Anush Krishna Moorthy and Alan Conrad Bovik, "Blind image quality assessment: From natural scene statistics to perceptual quality," *IEEE Transactions on Image Processing*, vol. 20, no. 12, pp. 3350–3364, 2011.
- [6] Jingtao Xu, Peng Ye, Qiaohong Li, Haiqing Du, Yong Liu, and David Doermann, "Blind image quality assessment based on high order statistics aggregation," *IEEE Transactions on Image Processing*, vol. 25, no. 9, pp. 4444–4457, 2016.
- [7] Chunyi Li, Zicheng Zhang, Haoning Wu, Wei Sun, Xiongkuo Min, Xiaohong Liu, Guangtao Zhai, and Weisi Lin, "Agiqa-3k: An open database for ai-generated image quality assessment," *IEEE Transactions on Circuits and Systems for Video Technology*, vol. 34, no. 8, pp. 6833–6846, 2024.
- [8] Chunyi Li, Jianbo Zhang, Zicheng Zhang, Haoning Wu, Yuan Tian, Wei Sun, Guo Lu, Xiaohong Liu, Xiongkuo Min, Weisi Lin, and Guangtao Zhai, "R-bench: Are your large multimodal model robust to real-world corruptions?," 2024.
- [9] Yang Liu, Weixing Chen, Yongjie Bai, Xiaodan Liang, Guanbin Li, Wen Gao, and Liang Lin, "Aligning cyber space with physical world: A comprehensive survey on embodied ai," 2024.
- [10] Brian Reily, Peng Gao, and Wang Hao Zhang, "Real-time recognition of team behaviors by multisensory graph-embedded robot learning," *International Journal of Robotics Research*, vol. 41, no. 8, pp. 798–811, 2022.
- [11] Xin. Zhou, Xiangyong. Wen, Zhepei. Wang, Yuman. Gao, Haojia. Li, Qianhao. Wang, Tiankai. Yang, Haojian. Lu, Yanjun. Cao, and Chao. Xu, "Swarm of micro flying robots in the wild," *Science robotics*, vol. 7, no. 66, pp. eabm5954, 2022.
- [12] Chunxu Li, Shuo Zhu, Zhongbo Sun, and James Rogers, "Bas optimized elm for kuka iiwa robot learning," *IEEE Transactions on Circuits and Systems II: Express Briefs*, vol. 68, no. 6, pp. 1987–1991, 2021.
- [13] Sami Haddadin, Sven Parusel, Lars Johannsmeier, Saskia Golz, Simon Gabl, Florian Walch, Mohamadreza Sabaghian, Christoph Jähne, Lukas Hausperger, and Simon Haddadin, "The franka emika robot: A reference platform for robotics research and education," *IEEE Robotics & Automation Magazine*, vol. 29, no. 2, pp. 46–64, 2022.
- [14] Viktor Makovychuk, Lukasz Wawrzyniak, Yunrong Guo, Michelle Lu, Kier Storey, Miles Macklin, David Hoeller, Nikita Rudin, Arthur Allshire, and Ankur Handa, "Isaac gym: High performance gpu-based physics simulation for robot learning," 2021.
- [15] N. Koenig and A. Howard, "Design and use paradigms for gazebo, an open-source multi-robot simulator," in *2004 IEEE/RSJ International Conference on Intelligent Robots and Systems (IROS) (IEEE Cat. No.04CH37566)*, 2004, vol. 3, pp. 2149–2154 vol.3.
- [16] Erwin Coumans and Yunfei Bai, "Pybullet, a python module for physics simulation for games, robotics and machine learning," 2016.
- [17] Eric Kolve, Roozbeh Mottaghi, Daniel Gordon, Yuke Zhu, Abhinav Gupta, and Ali Farhadi, "AI2-THOR: an interactive 3d environment for visual AI," *CoRR*, vol. abs/1712.05474, 2017.
- [18] Manolis Savva, Abhishek Kadian, Aleksandr Maksymets, Yili Zhao, Erik Wijmans, Bhavana Jain, Julian Straub, Jia Liu, Vladlen Koltun, Jitendra Malik, Devi Parikh, and Dhruv Batra, "Habitat: A platform for embodied ai research," in *2019 IEEE/CVF International Conference on Computer Vision (ICCV)*, 2019, pp. 9338–9346.
- [19] Fanbo Xiang, Yuzhe Qin, Kaichun Mo, Yikuan Xia, Hao Zhu, Fangchen Liu, Minghua Liu, Hanxiao Jiang, Yifu Yuan, He Wang, Li Yi, Angel X. Chang, Leonidas J. Guibas, and Hao Su, "Sapien: A simulated part-based interactive environment," in *2020 IEEE/CVF Conference on Computer Vision and Pattern Recognition (CVPR)*, 2020, pp. 11094–11104.
- [20] John Schulman, Filip Wolski, Prafulla Dhariwal, Alec Radford, and Oleg Klimov, "Proximal policy optimization algorithms," *arXiv preprint arXiv:1707.06347*, 2017.
- [21] Tuomas Haarnoja, Aurick Zhou, Kristian Hartikainen, George Tucker, Sehoon Ha, Jie Tan, Vikash Kumar, Henry Zhu, Abhishek Gupta, Pieter Abbeel, et al., "Soft actor-critic algorithms and applications," *arXiv preprint arXiv:1812.05905*, 2018.
- [22] Nicklas Hansen, Hao Su, and Xiaolong Wang, "Td-mpc2: Scalable, robust world models for continuous control," *arXiv preprint arXiv:2310.16828*, 2023.
- [23] Stone Tao, Fanbo Xiang, Arth Shukla, Yuzhe Qin, Xander Hinrichsen, Xiaodi Yuan, Chen Bao, Xinsong Lin, Yulin Liu, Tse kai Chan, Yuan Gao, Xuanlin Li, Tongzhou Mu, Nan Xiao, Arnav Gurha, Zhiao Huang, Roberto Calandra, Rui Chen, Shan Luo, and Hao Su, "Maniskill3: Gpu parallelized robotics simulation and rendering for generalizable embodied ai," *arXiv preprint arXiv:2410.00425*, 2024.
- [24] Shanshan Lao, Yuan Gong, Shuwei Shi, Sidi Yang, Tianhe Wu, Jiahao Wang, Weihao Xia, and Yujiu Yang, "Attentions help cnns see better: Attention-based hybrid image quality assessment network," in *Proceedings of the IEEE/CVF conference on computer vision and pattern recognition*, 2022, pp. 1140–1149.
- [25] Ekta Prashnani, Hong Cai, Yasamin Mostofi, and Pradeep Sen, "Pieapp: Perceptual image-error assessment through pairwise preference," in *Proceedings of the IEEE Conference on Computer Vision and Pattern Recognition*, 2018, pp. 1808–1817.
- [26] Heliang Zheng, Huan Yang, Jianlong Fu, Zheng-Jun Zha, and Jiebo Luo, "Learning conditional knowledge distillation for degraded-reference image quality assessment," in *Proceedings of the IEEE/CVF International Conference on Computer Vision*, 2021, pp. 10242–10251.
- [27] Keyan Ding, Kede Ma, Shiqi Wang, and Eero P. Simoncelli, "Image quality assessment: Unifying structure and texture similarity," *IEEE Transactions on Pattern Analysis and Machine Intelligence*, vol. 44, no. 5, pp. 2567–2581, 2022.
- [28] Chaofeng Chen, Jiadi Mo, Jingwen Hou, Haoning Wu, Liang Liao, Wenxiu Sun, Qiong Yan, and Weisi Lin, "Topiq: A top-down approach from semantics to distortions for image quality assessment," *IEEE Transactions on Image Processing*, vol. 33, pp. 2404–2418, 2024.
- [29] Manri Cheon, Sung-Jun Yoon, Byungyeon Kang, and Junwoo Lee, "Perceptual image quality assessment with transformers," in *2021 IEEE/CVF Conference on Computer Vision and Pattern Recognition Workshops (CVPRW)*, 2021, pp. 433–442.
- [30] Jianyi Wang, Kelvin CK Chan, and Chen Change Loy, "Exploring clip for assessing the look and feel of images," in *Proceedings of the AAAI Conference on Artificial Intelligence*, 2023, vol. 37, pp. 2555–2563.
- [31] Weixia Zhang, Kede Ma, Jia Yan, Dexiang Deng, and Zhou Wang, "Blind image quality assessment using a deep bilinear convolutional neural network," *IEEE Transactions on Circuits and Systems for Video Technology*, vol. 30, no. 1, pp. 36–47, 2020.
- [32] Sidi Yang, Tianhe Wu, Shuwei Shi, Shanshan Lao, Yuan Gong, Mingdeng Cao, Jiahao Wang, and Yujiu Yang, "Maniqa: Multi-dimension attention network for no-reference image quality assessment," in *Proceedings of the IEEE/CVF Conference on Computer Vision and Pattern Recognition*, 2022, pp. 1191–1200.
- [33] Jinsong Shi, Pan Gao, and Aljosa Smolic, "Blind image quality assessment via transformer predicted error map and perceptual quality token," *IEEE Transactions on Multimedia*, vol. 26, pp. 4641–4651, 2024.
- [34] Shaolin Su, Qingsen Yan, Yu Zhu, Cheng Zhang, Xin Ge, Jinqu Sun, and Yanning Zhang, "Blindly assess image quality in the wild guided by a self-adaptive hyper network," in *Proceedings of the IEEE/CVF conference on computer vision and pattern recognition*, 2020, pp. 3667–3676.
- [35] Chaofeng Chen and Jiadi Mo, "IQA-PyTorch: Pytorch toolbox for image quality assessment," [Online]. Available: <https://github.com/chaofengc/IQA-PyTorch>, 2022.